Study of Dispersion Morphologies of Isotactic Polypropylene and Linear Low Density Polyethylene Blends by Scanning Electron Microscopy

YAN LIU and ROWAN W. TRUSS*

Department of Mining and Metallurgical Engineering, The University of Queensland, St. Lucia, Queensland 4072, Australia

SYNOPSIS

Isotactic polypropylene (iPP) and linear low-density polyethylene (LLDPE) blends with five different component ratios were prepared by melt mixing. The blends were subsequently remelted at 200°C for 1, 2, 3, 5, 8, 12, 20 min, and 2 h. The morphologies of the heat-treated and as-blended materials were studied on the cryogenically fractured surfaces of these blends by scanning electron microscopy (SEM). It was found that the morphologies of the blends with equal component ratio were highly unstable in remelting, while those blends with the lowest minor component ratios were the most stable ones, showing a growth in the size of the dispersed particles. © 1996 John Wiley & Sons, Inc.

INTRODUCTION

Polymer blends are of considerable interest for recycling plastic waste, in which plastics of different polymer types are mixed to form reuseable materials with acceptable properties. They are also important for improving the properties of virgin materials, such as impact strength and tensile strength.[1] The present work has been focused on the mechanical properties and microstructures of the blends of isotactic polypropylene (iPP) and linear low density polyethylene (LLDPE).[2] This work is motivated by the facts that iPP and LLDPE are among the most commonly used plastics and in recycle processing, are generally sorted into the stream of polyolefin from the mixed waste.

Polymers of iPP and LLDPE are immiscible with each other[2] and, thus, they are microscopically separated in the blends. Generally, one of them, depending on the ratio between the two components of the blend, is dispersed rather than dissolved in the matrix of the other.[3,4] For a blend consisting of two immiscible polymers, there are two important factors that affect the mechanical properties of the blend:[5-9] the morphology of the dispersed polymer and the interfacial adhesion between the dispersoids and the matrix. For a macroscopically homogenous blend, for example, the dispersoids have to be fine and be uniformly distributed, while, for retaining the integrity of a blend in application, the interfacial adhesion has to be strong enough to sustain the stress developed. In order to improve the interfacial adhesion, compatibilisers can be added to the blends to mediate an attractive interaction between the immiscible polymer components.[10]

The morphology of the dispersed polymer affects the mechanical properties of the blend, e.g., elasticity, yield strength, impact strength, and ultimate tensile strength.[11-16] For example, large particle size and weak adhesion would result in poor mechanical properties in the blends of polyolefins.[2,17]

The morphology of finely dispersed components in immiscible blends can be considered to be a result of the balance between two concurrent processes occurring in blending:[18,19] the coalescence between the dispersoids upon collision due to random Brownian motion and/or interparticle attractions (e.g., van der Waals forces and electrostatic forces); and the deformation and breaking up of the dispersed polymer by the means used in the blending process such as shearing. To obtain a blend of desired dispersion morphology both the initial proportion of the poly-

* To whom correspondence should be addressed.

Journal of Applied Polymer Science, Vol. 60, 1461–1473 (1996)
 CCC 0021-8995/96/091461-13

mers in the blend and the blending procedures have to be carefully controlled. It has been found[18] that the coalescence effect could be impeded by lowering the portion of the dispersed polymer in the blend. The dispersoid size has been found to increase linearly with the portion of the dispersed polymer when the portion is low.[20,21]

When a blend is left in its molten state, there is no longer a balance between the coalescence and break-up process, but coalescence dominates. The coalescence process resulting from collision between dispersoids due to Brownian motion in immiscible binary blends has been dealt with theoretically by Smoluchowski.[22–25] Furthermore, for a system of dispersed monospherical particles, it was found by Fortelny and Kovar[26,27] that the inverse of the square root of the number of particles per unit volume (n) is proportional to the square root of the time (t) for which the coalescence has occurred such that

$$\left(\frac{1}{n}\right)^{1/2} = 4\left(\frac{kT\phi}{\pi\eta}\right)^{1/2} t^{1/2} + \left(\frac{1}{n_0}\right)^{1/2} \quad (1)$$

where n_0 is the initial number of spheres per unit area, k the Boltzmann constant, T the melt temperature, η viscosity of matrix polymer, and ϕ the volume fraction of the dispersed polymer component.

For iPP/LLDPE blends, it has been found that their mechanical and thermal properties depended not only on the component proportions, but also on the crystallinity, the mechanical, and thermal properties of each component,[28,29] the morphology of the dispersoid, and the interfacial bonding between the two components.[30,31] The blending and manufacturing processes were found important to the dispersion morphology[32–34] and also to the mechanical properties of the blends.[35,36] However, the stability of the morphology of the dispersoids in the blends of iPP/LLDPE is still not well known, although the morphological stability of the dispersoid is crucial to the reproducibility of the properties of the blends and their performance in application.

In our earlier work concerning the relationship between the mechanical properties and microstructures of the blends of iPP/LLDPE, all the tensile test specimens used were prepared by hot pressing of blends obtained with a twin-blade mixer.[2] Because the morphology of the dispersed particles in the blends is an important aspect of the blends that influences the properties and applications of the materials, it is worthwhile to conduct an investigation into the morphological stability of the dispersion of these blends. In the present work, the effect of remelting on the morphological stabilities of the dispersoids in the iPP/LLDPE blends was studied by scanning electron microscopy (SEM). It has been found that the morphology of the blends was generally stable except for the one with equal weight proportion of components whose morphology changed dramatically during the first few minutes of remelting.

EXPERIMENTAL

The iPP and LLDPE used in this study were grade GXM43 and FG414, respectively, supplied by ICI, Australia Plastics Group. They were originally in the form of extruded pellets. These pellets were later mixed to form blends at the following weight proportions: 90% iPP to 10% LLDPE (90PP/10LLDPE), 75% iPP to 25% LLDPE (75PP/25LLDPE), 50% iPP to 50% LLDPE (50PP/50LLDPE), 25% iPP to 75% LLDPE (25PP/75LLDPE), and 10% iPP to 90% LLDPE (10PP/90LLDPE). The equipment used for blending was a twin-blade mixer, Brabender, Plasti-Corder PL2000. The mixed pellets were blended at 200°C for 5 min with a blade speed of 60 rpm. The molten blends were then taken out from the mixer and pressed between two 3 mm thick Al plates to form small blocks[2] referred to as as-blended samples.

Specimens from the as-blended samples were wrapped in Al foil and then remelted in an oven at 220°C for respectively 20 min and 2 h. After the remelting, the blends were taken out of the oven and air cooled to room temperature. After finding that the morphology of the 50PP/50LLDPE sample changed dramatically from that of the as-blended one after remelting, the 50PP/50LLDPE as-blended specimens were remelted at 200°C for time intervals: 1, 2, 3, 5, 8, 12, 20 min, and 2 h and then quenched in water to room temperature.

For SEM investigation, all of the above heat-treated specimens together with the as-blended specimens were fractured in liquid nitrogen. In order to confine the initiation position for cracking, a shallow notch was made on the surface of each specimen with a scalpel. The specimen was submerged in liquid nitrogen for about 25 min before fracturing by impact. The fractured surfaces were then carbon coated and investigated in an SEM instrument, JEOL 6400, operating at 5 kV. The SEM micrographs shown in this article are all secondary electron images.

In order to compare the viscosity values of iPP and LLDPE matrices of the blends, the viscosities of pure iPP and LLDPE specimens were measured using a Rheometrics mechanical spectrometer/Dynamic spectrometer RMS-800/RDS II at 220°C. Cone-plate geometry with a cone angle of 0.02 rad was used. The zero shear viscosity η_0 of each specimen was obtained from the curve fitting of the data of measured viscosity η as a function of dynamic sweep frequency ω (proportional to shear rate $\dot{\gamma}$) with the Carreau equation:[37]

$$\eta = \eta_0[1 + (\tau^*\dot{\gamma})^2]^{-m} \quad (2)$$

where τ^* and m are experimental constants.

RESULTS AND DISCUSSION

Fractography of the Blends

The topography of the fractured surfaces of the blends varied notably, depending on the relative distance from the shallow notch made for the crack initiation. As an example, Figure 1 shows SEM images taken from the fractured surface of an as-blended 10PP/90LLDPE specimen with the general view shown in (a) and detailed views of the regions B, C, and D, as indicated in (a) shown in (b), (c), and (d), respectively. Region A in Figure 1(a) is the notch made for crack initiation. As can be seen, adjacent to the notch the fractured surface was of brittle fracture nature (region B) because the crack cut through both the LLDPE matrix and the iPP dispersed particles without leaving traces of drawing. When it was far from the notch, even though the specimen had been kept in liquid nitrogen for 25 min before fracturing, the fractured surface had certain ductile fracture features (regions C and D) where the LLDPE left on the fractured surface was drawn and iPP particles were either fractured or debonded from the matrix. In this work, the morphology of the dispersed particles was studied by examining the brittle fractures [e.g., Fig. 1(b)] because of the ease of microstructural interpretation from such regions.

It is worth mentioning here that, besides the features of brittle and ductile fractured surfaces, a bright flake-like contrast present in regions B and C in Figure 1(a) was seen in some of the specimens. At higher magnifications, however, no particular difference in topography was found corresponding to this pattern of contrast. The topography of such regions was similar to that of region B. The nature of this patten is still not known. It is speculated that it might be due to the presence of certain structural inhomogeneity, the fractured surface of which would give rise to different yields of secondary electrons. However, the structure on the fractured surface of such inhomogeneity would have been too fine to be resolved by the present SEM.

Morphology Stability of Blends of 90PP/10LLDPE, 75PP/25LLDPE, 25PP/75LLDPE, and 10PP/90LLDPE

Except for the blend of 50PP/50LLDPE (which was found highly unstable and will be shown in the next section), the morphology of the dispersions in the rest of the blends prepared in this study was found to have changed only slightly after the remelting treatment. In Figures 2 to 5, SEM images reveal the fractured surfaces of the blends of 90PP/10LLDPE, 75PP/25LLDPE, 25PP/75LLDPE, and 10PP/90LLDPE, respectively. In each of these figures, (a) is of the as-blended, (b) after 20 min of remelting, and (c) after 2 h of remelting. As can be seen from the micrographs of the as-blended specimens, in general, the dispersoids were spherical, apart from some of those in the blend of 25PP/75LLDPE, which became spherical after the remelting treatments [Figs. 4(b) and (c)]. The dispersoids were considered to be LLDPE in the blends with 90% and 75% of iPP and to be iPP in the blends with 25% and 10% of iPP. This consideration was consistent with experimental observation that the apparent volume fraction of the dispersoids increased with iPP proportion when less than 50% and decreased with iPP proportion when larger than 50%. Moreover, on the fractured surfaces, LLDPE generally showed more drawn features than iPP. In Figures 2 and 3, which corresponded to the blends of 90PP/10LLDPE, and 75PP/25LLDPE, respectively, the dispersoids could be recognized as domes and spherical hollows on the fractured surfaces. These features could result from interfacial debonding during fracturing. By way of contrast, most of the dispersoids in the blends of 25PP/75LLDPE and 10PP/90LLDPE (Figs. 4 and 5) were sectioned by the crack during fracturing.

After the remelting treatment, as can be seen in Figures 2 to 5, the number of the dispersoids seemed to decrease and the size of them to increase more evidently in the blends of 75PP/25LLDPE and 25PP/75LLDPE than in the blends of 90PP/10LLDPE and 10PP/90LLDPE. This indicated that the dispersoids in the blends were coarsened during remelting. In order to assess this coarsening

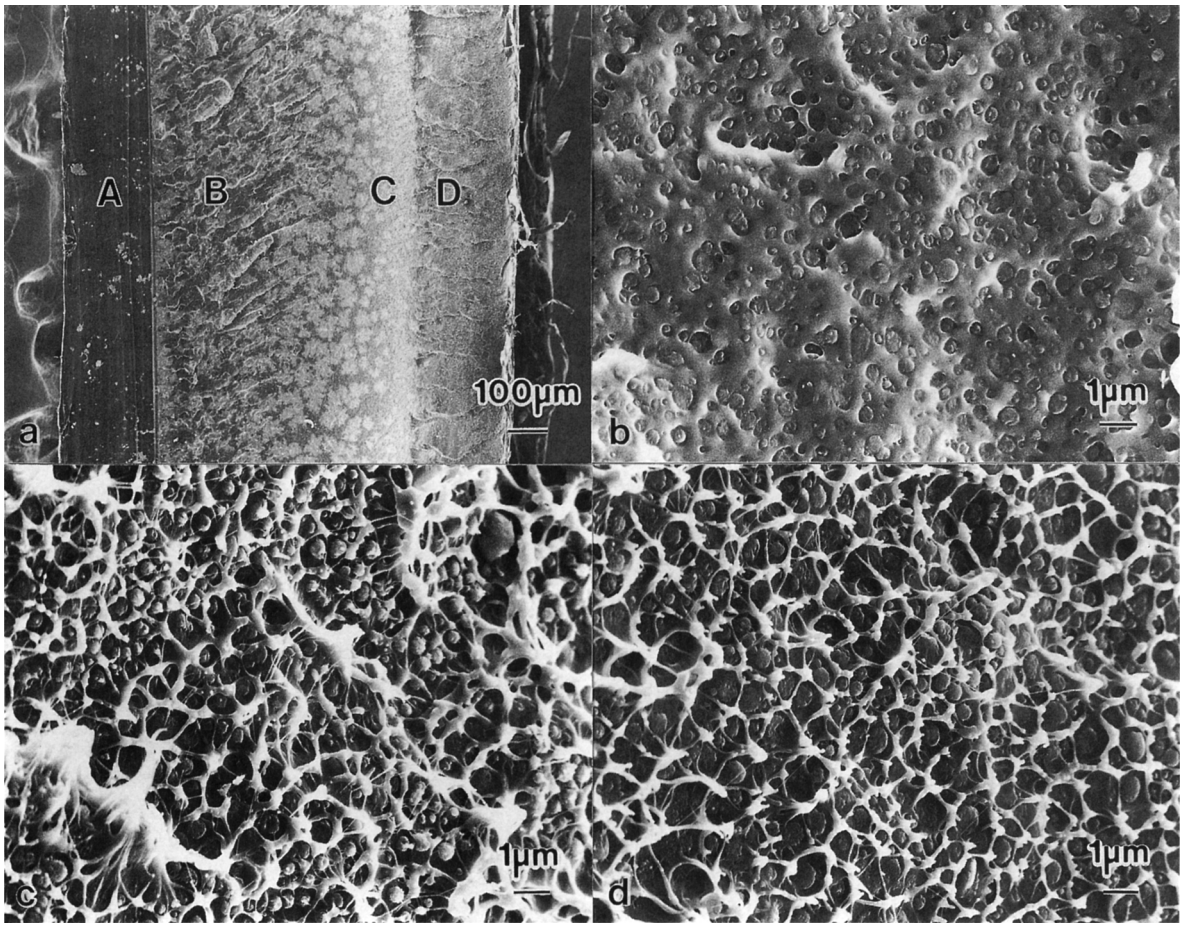

Figure 1 SEM images showing typical fracture topographies of an as-blended 10PP/90LLDPE blend: (a) an overview of the specimen; and (b), (c), and (d), respectively, the detailed views of the regions of B, C, and D, as indicated in (a). Region B showed a brittle fracture morphology, while regions C and D showed ductile fractures.

effect, a measurement of the number of dispersed particles found per unit area of the fractured surface for these blends as a function of remelting time was conducted. The measurement was conducted by counting the number of dispersoids per SEM image at a magnification of 5,000 times corresponding to a field about 365 μm^2 on the fractured surface. For each specimen, at least two images from the same specimen were measured and the average deviation between the counts from the different SEM images was about 10%. Figure 6 is a plot showing the results of this measurement. In Figure 6(a), the number of dispersoids counted was plotted as a function of remelting time, while in Figure 6(b) the number of dispersoids were normalized (i.e., the number of dispersoids is divided by the number found in the as-blended specimen of the same blend) to show the stability of the dispersion. From the plots shown in Figure 6, it can be seen that coarsening of the dispersoids had occurred in all these four blends, with the reduction in number of dispersoids being more evident in the first 20 min of remelting. The 90PP/10LLDPE and 10PP/90LLDPE blends were more stable in remelting than the blends of 75PP/25LLDPE and 25PP/75LLDPE [Fig. 6(b)]. In the former two blends, the number of dispersoids reduced to about 70% of their original number after 2 h of remelting, while in the latter two blends the number reduced to only about 40% of their original count. It can also be noted that among the as-blended specimens, the former two blends had higher numbers of dispersoids per unit area than the latter two, with the 90PP/10LLDPE having the highest number.

It is interesting to note that, regardless of the remelting treatment and the species of dispersoids in the blends, the areal fractions of dispersoids (which represent the volume fractions of the dis-

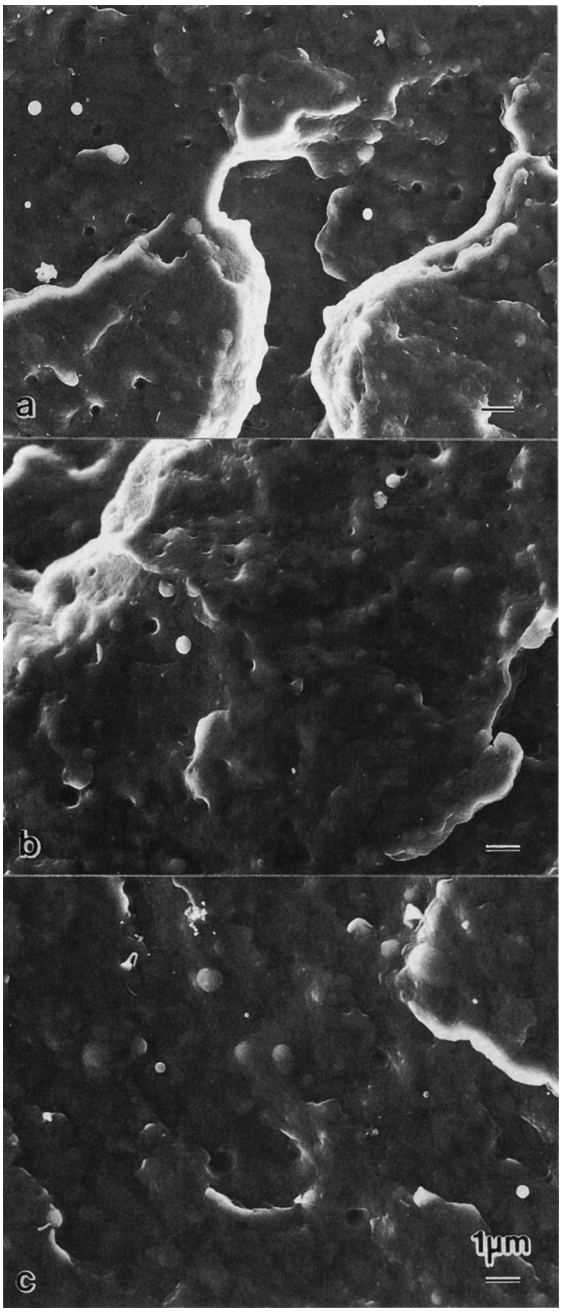

Figure 2 SEM micrographs of the fractured surfaces of a 90PP/10LLDPE blend showing typical dispersion morphologies of the blend after different heat treatment: (a) as-blended, (b) remelted for 20 min, and (c) remelted for 2 h.

persoids in the blends) found on the fractured surfaces appeared to be higher than expected in the blends. This may perhaps have been because the crack tended to develop across the diameter of the spherical dispersoids during fracturing, giving an impression that the volume fraction was higher than it was in reality. It may also have resulted because the dispersoids and also the matrix in their vicinities were all heavily deformed during fracturing such that they appeared larger than they actually were in SEM.

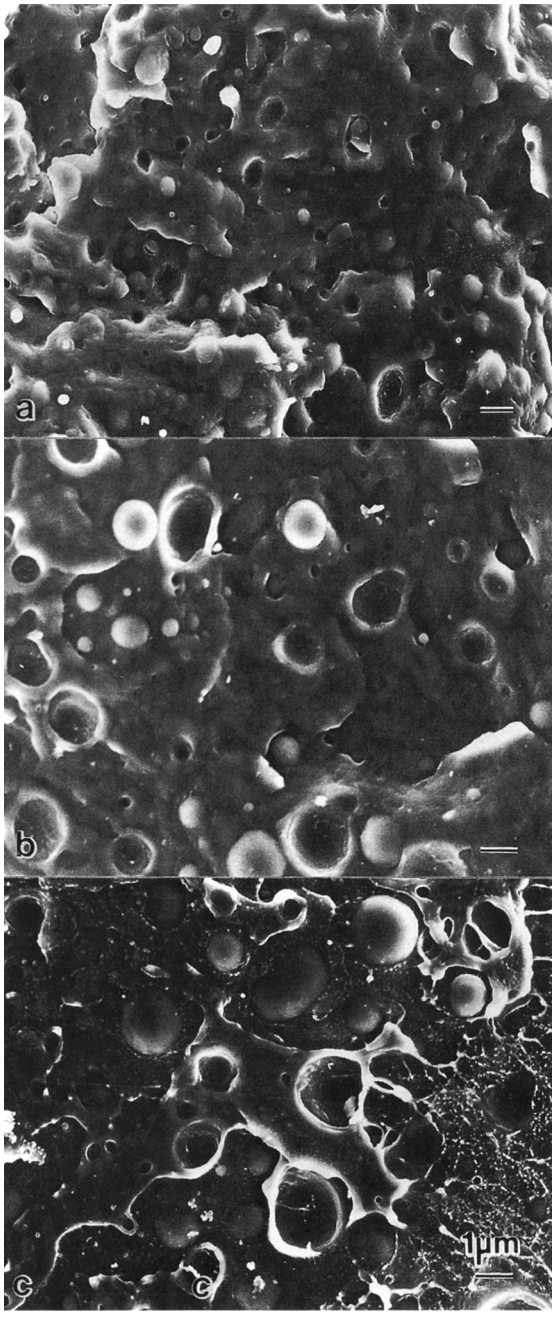

Figure 3 SEM micrographs of the fractured surfaces of a 75PP/25LLDPE blend showing typical dispersion morphologies of the blend after different heat treatment: (a) as-blended, (b) remelted for 20 min, and (c) remelted for 2 h.

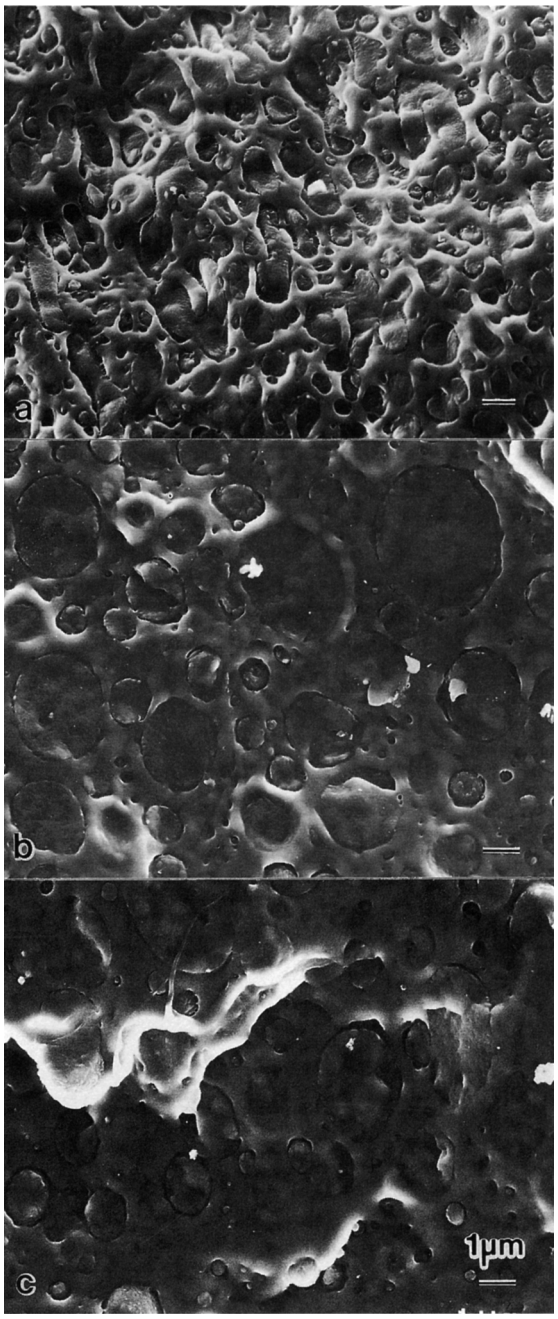

Figure 4 SEM micrographs of the fractured surfaces of a 25PP/75LLDPE blend showing typical dispersion morphologies of the blend after different heat treatment: (a) as-blended, (b) remelted for 20 min, and (c) remelted for 2 h.

An attempt was made in this study to analyze the coalescence process of these blends using eq. (1), a theoretical result obtained by Fortelny and Kovar.[27] As an approximation, it was assumed that $n = (n_a)^{3/2}$, where n is the number of particles per unit volume and n_a was number of particles per unit area counted on the fractured surface. Using this assumption, data shown in Figure 6 were replotted in Figure 7 in order to compare with eq. (1). Comparing with eq. (1), the linear dependence of $n^{-1/2}$ on $t^{1/2}$ can be seen in the two blends with lower minor components, while deviation from this can

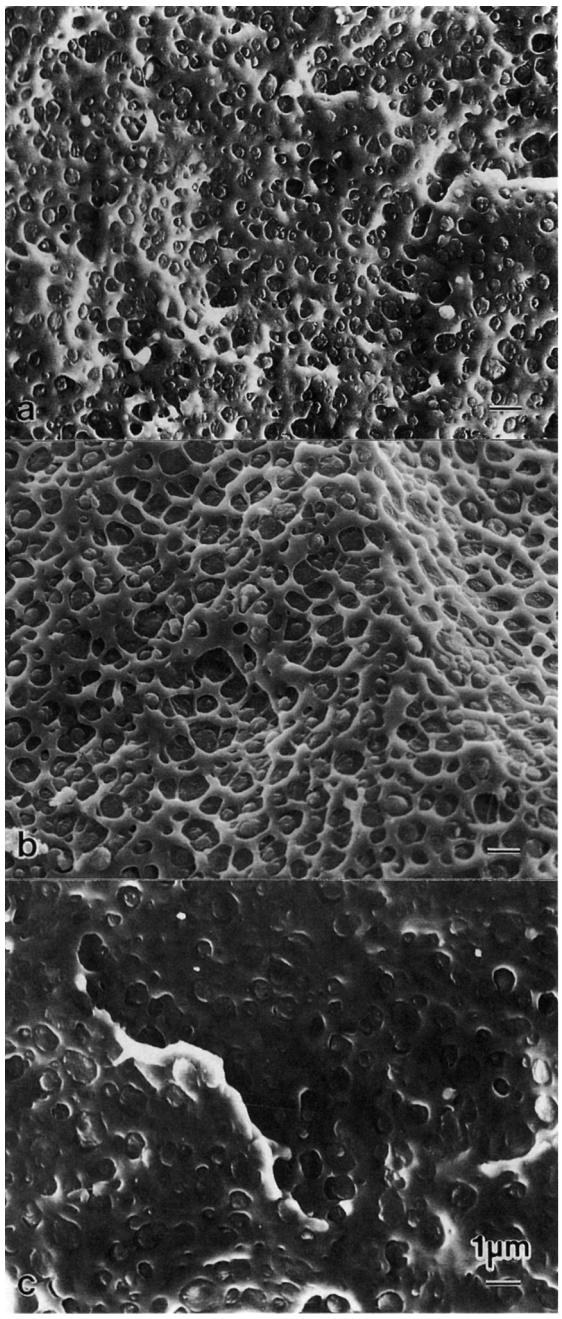

Figure 5 SEM micrographs of the fractured surfaces of a 10PP/90LLDPE blend showing typical dispersion morphologies of the blend after different heat treatment: (a) as-blended, (b) remelted for 20 min, and (c) remelted for 2 h.

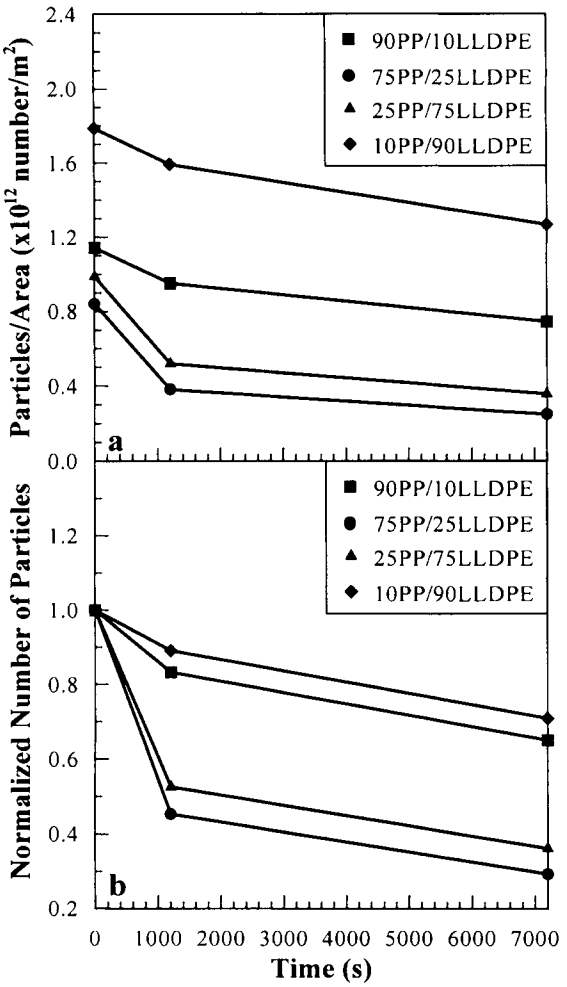

Figure 6 Plots of the number of particles counted from the fractured surfaces of iPP/LLDPE blends (whose component ratios are indicated in the plot) as a function of the remelting time: (a) the number of particles per unit area and (b) the normalized number of particles per unit area.

be seen for the two blends with high minor components. The increase in the slope of the curves with increase in the minor component can be seen between both the 90PP/10LLDPE and 75PP/25LLDPE blends and the 10PP/90LLDPE and 25PP/75LLDPE. Note that eq. (1) was derived assuming that Brownian motion of the individual particles does not affect each other and, thus, it is valid only in dilute systems. Thus, the deviation from the linear dependence for the two high minor component blends could be due to deviation from the assumptions of the theory.

A further attempt was made to calculate the viscosity of the matrix material of these blends using eq. (1) with the data shown in Figure 7. The results of this calculation are shown in Table I. For comparison, also shown in Table I are the results of zero-shear viscosity of the pure iPP and LLDPE calculated using eq. (2) to best fit the plots from viscosity measurement shown in Figure 8.

As can be seen in Table I, for the blends, the viscosity of iPP in general was 1 ~ 2 times smaller than that of LLDPE matrix with the same weight fraction of dispersoids. When the weight fraction increased, the measured viscosity of the matrix material decreased about an order of magnitude. It is obvious that the calculated viscosity of matrix component was greatly influenced by the concentration of dispersoids. This is not surprising, because the blends with 25% weight fraction of dispersoid cannot be regarded as diluted systems to which eq. (1) applies. This was reflected in the nonlinear dependence of $n^{-1/2}$ on $t^{1/2}$ for those blends (Fig. 7). The 10% weight fraction blends showed a linear dependence of $n^{-1/2}$ on $t^{1/2}$ that seemed to suggest that these blends could be treated as dilute systems. However, when compared with the corresponding values of zero shear viscosity, the viscosities of the matrices of these blends were still an order of magnitude smaller. There could be a number of reasons to account for this discrepancy: (1) Brownian motion would induce shear field around each particle and, thus, the local viscosity of the matrix for the particle would be reduced, because the viscosity of the matrix materials decreases with shear rate. This shear-rate dependence of the viscosity was not included in the Fortelny and Kovar's theory. (2) It is possible that some degradation of the polymer may have occurred

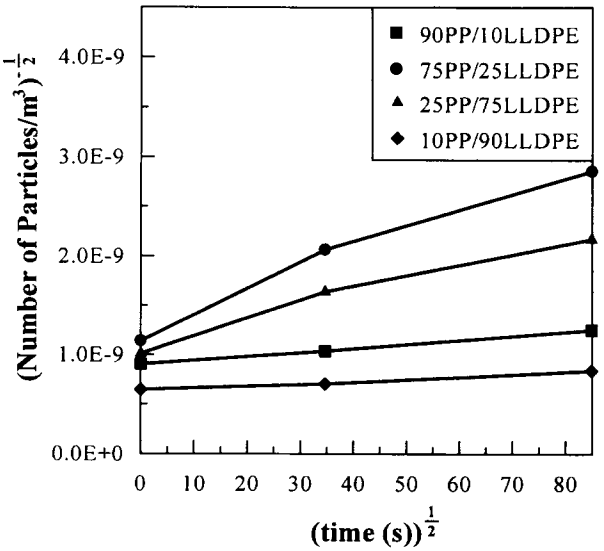

Figure 7 The number of particles per equivalent unit volume as a function of remelting time.

Table I Viscosities Calculated from Coarsening of the Dispersed Blends and Measured Viscosity of Pure iPP and LLDPE

Material		Viscosity (Pa s)	Note
iPP	75PP/25LLDPE	22	From eq. (1)
	90PP/10LLDPE	208	From eq. (1)
	Pure iPP	3757	Zero-shear, from eq. (2)
LLDPE	25PP/75LLDPE	48	From eq. (1)
	10PP/90LLDPE	669	From eq. (1)
	Pure LLDPE	7710	Zero-shear, from eq. (2)

during the long-time remelting treatment. In the case of iPP at least, the viscosity would be expected to decrease with degradation but probably not as much as an order of magnitude. Moreover, any reduction in viscosity as a result of degradation would have occurred over time causing nonlinearity in the plot of Figure 8. (3) Because the fracture surfaces were not ideally flat, errors may have resulted in the particle density measurement and a consequential effect on the viscosity measurement. (4) However, the most likely explanation is that the 10% weight fraction is still not low enough for the blends to be considered satisfactorily as dilute systems.

Morphology Stability of 50PP/50LLDPE

The blend of 50PP/50LLDPE was found to be highly unstable in the remelting treatment. The specimens of this blend became whitened due to the formation of pores after remelting, as shown in Figure 9. After remelting for 2 h, the pores became so large that they could be clearly seen optically in the center region of the specimen (specimen C in Fig. 9). The edge region of both of the remelted specimens appeared more transparent than the as-blended specimen. This seemed to be because these regions were very thin after the prolonged remelting and, thus, pores formed in such regions had a higher possibility to be in contact with the specimen surfaces than those formed in the interior of thicker regions. Once a pore is in contact with the specimen surface, it would be soon annihilated. The annihilation of pores at the specimen surface would reduce the total amount of pores and would increase the transparency in the material.

Figure 10 presents the fractured surfaces of this blend from different remelting stages: (a) as-blended, (b) remelted for 20 min, and (c) remelted for 2 h. In the as-blended 50PP/50LLDPE specimen [Fig. 10(a)], iPP and LLDPE were lamella like, resulting from the shearing process of blending. Af-

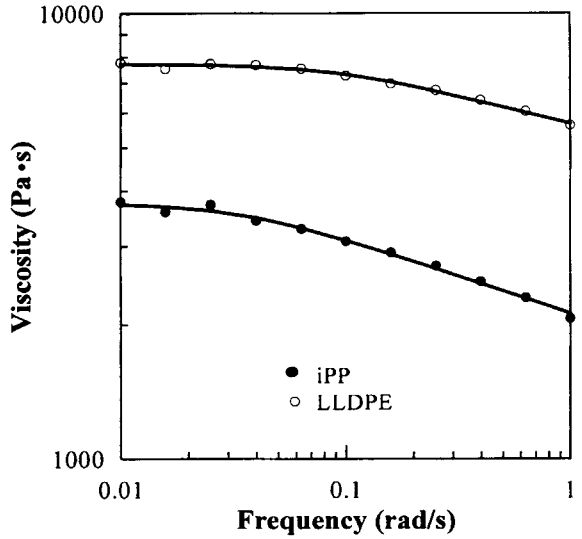

Figure 8 Shear dependent viscosity of iPP (dot) and LLDPE (circle) at 220°C. The solid lines are the best fit of eq. (2) (Carreau equation).

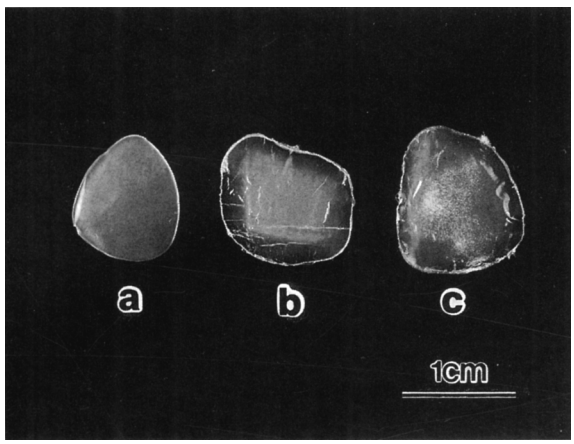

Figure 9 Optical photographs showing blend specimens of 50PP/50LLDPE after being remelted for (a) 1 min, (b) 20 min, and (c) 2 h.

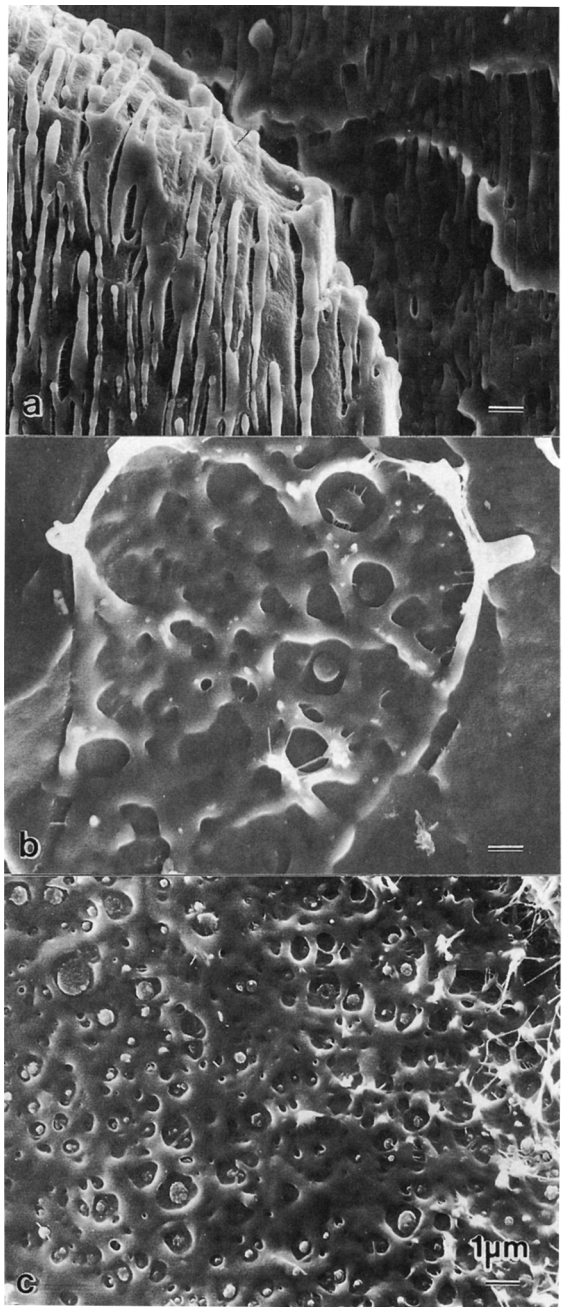

Figure 10 SEM micrographs of the fractured surfaces of a 50PP/50LLDPE blend showing typical dispersion morphologies of the blend after different heat treatment: (a) as-blended, (b) remelted for 20 min, and (c) remelted for 2 h.

ter the specimen was remelted for 20 min, the lamella-like morphology had disappeared and dramatic coalescence had taken place in the blend forming iPP/LLDPE complexes and pores in the matrix of iPP. Regions presented by the micrographs in Figure 10(b) and (c) were, respectively, a part of a complex surrounded by iPP matrix and a part of a complex. No obvious further coalescence of iPP particles within the complex was observed. Figure 11 presents another view of the coalescence process for this blends where the magnification was varied between micrographs in order to show an overview of the process. The lamella-like morphology can again be seen here in Figure 11(a), where the LLDPE lamellae were drawn during fracturing and iPP lamellae were interconnected as a matrix holding the lamellae of LLDPE. The above-mentioned iPP/LLDPE complexes, pores, and iPP matrix are indicated respectively by "C," "P," and "M" in Figure 11(b) and (c). On the fractured surfaces, the open pores appeared smooth, the iPP/LLDPE complex, in which spherical iPP particles were embedded in the domains of LLDPE [shown in some detail in Fig. 10(b) and (c)] showed network-like features from the drawn LLDPE, and iPP matrix had a brittle fracture morphology that appeared dark. The topography of the blend specimen remelted for 2 h was similar to that remelted for 20 min [Fig. 11(b)], but coarser [note that the image magnification is 10 times larger in Fig. 10(c) than in 10(b)]. Apparently, the overall morphology of this blend after the 20 min remelting was domains of iPP/LLDPE complexes that were interconnected in the matrix of iPP and, thus, formed an interpenetrating network morphology with the domains of iPP as shown in Figure 12 and pores that formed and grew in size in between the iPP/LLDPE complex and iPP matrix. After the 2 h remelting, the interconnected domains of iPP/LLDPE complexes and the interpenetrating networks with the domains of iPP were further developed. The pores also grew further in size between the two types of domains.

In order to investigate the microstructural development of the 50PP/50LLDPE blend in detail, specimens from the as-blended sample were remelted at 200°C for 1, 2, 3, 5, 8, 12, 20 min, and 2 h and quenched in water to room temperature after remelting. The fractured surfaces of these specimens are shown by the SEM images in Figure 13. After 1 min remelting [Fig. 13(b)], the lamellae-like LLDPE became thickened and rounded as compared with those in the as-blended specimen [Fig. 13(a)]. Some iPP particles were entrapped in the LLDPE as the LLDPE particles coalesced forming the iPP/LLDPE complexes [as arrowed in Fig. 13(b)]. As the remelting treatment was continued, isolated LLDPE particles could rarely be seen [Fig. 13(a) to (i)]. This could be due to significant coalescence of LLDPE and iPP/LLDPE complexes. These

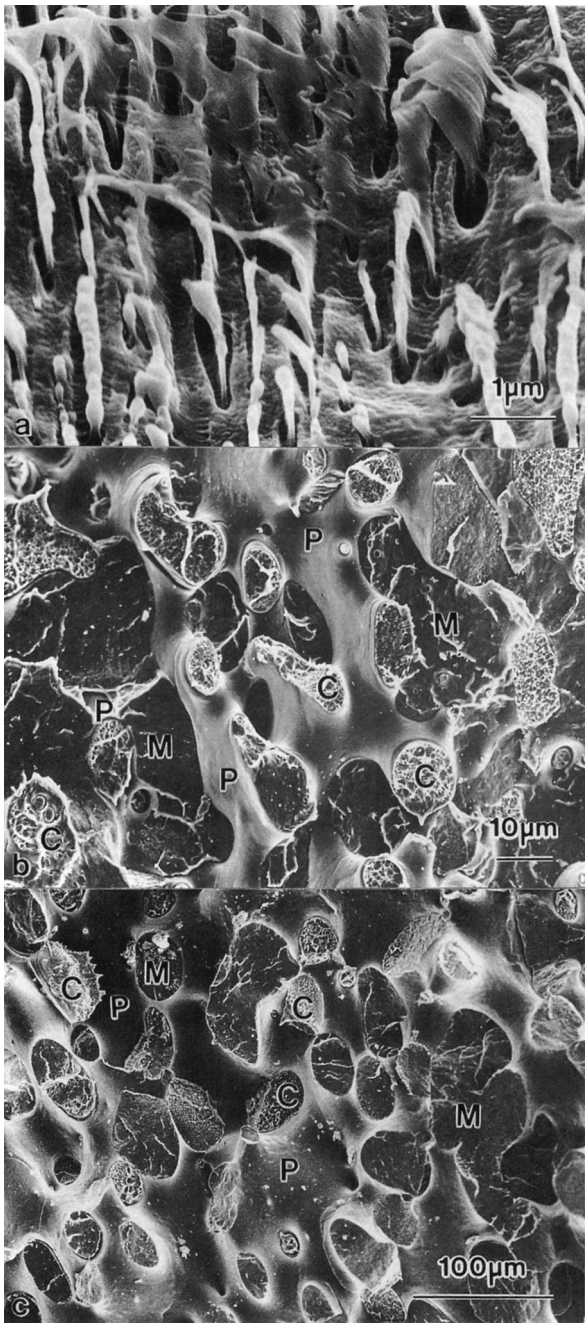

Figure 11 SEM images of the fractured surfaces of a 50PP/50LLDPE blend showing the coalescence process occurred in the blend after different heat treatment: (a) as-blended, (b) remelted for 20 min, and (c) remelted for 2 h.

complexes grew in size with remelting time. Pores started to appear at the interface between iPP and iPP/LLDPE complex after remelting for about 5 min [as indicated in Fig. 13(e)]. Recognizable pores are also indicated in Figure 13(f) to (h). The iPP particles in the complex were spherical because they had a disc-like morphology on the fractured surfaces. Examining the size of iPP particles in the complex as a function of remelting times, it can be seen that, although there were no significant size increases for the iPP particles with remelting time, larger iPP particles formed in the late stages of remelting treatment [Fig. 13(g) to (i)]. This size increase may result from possible coalescence of iPP particles in the complexes. However, further quantitative observation is needed in order to verify this consideration.

Evidently, in the blending process iPP and LLDPE in this 50PP/50LLDPE blend were sheared into a lamellae form and this morphology was not stable in the remelting treatment. During remelting, the LLDPE lamellae became thickened and rounded in the matrix of iPP under the influence of interfacial tension and coalescence between the LLDPE particles occurred. During coalescence, a small amount of iPP was trapped in LLDPE forming iPP/LLDPE complexes, whereas the majority of iPP served as a continuous matrix. This was probably because in the as-blended condition, iPP lamellae were interconnected [Figs. 10(a) and 11(a)]. The entrapment of iPP particles in LLDPE was recognizable even at the beginning of remelting treatment, as arrowed in Figure 13(b). In fact, this entrapment may have occurred only at the initial stage of coalescence when the lamellae of LLDPE became rounded under the influence of interfacial tension.

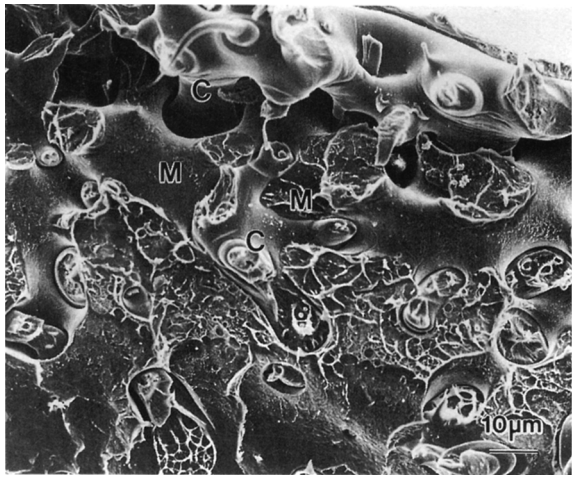

Figure 12 SEM images of the fractured surfaces of a 50PP/50LLDPE blend showing the interpenetrating between iPP and iPP/LLDPE complexes forming a network after the blend being remelted for 20 min.

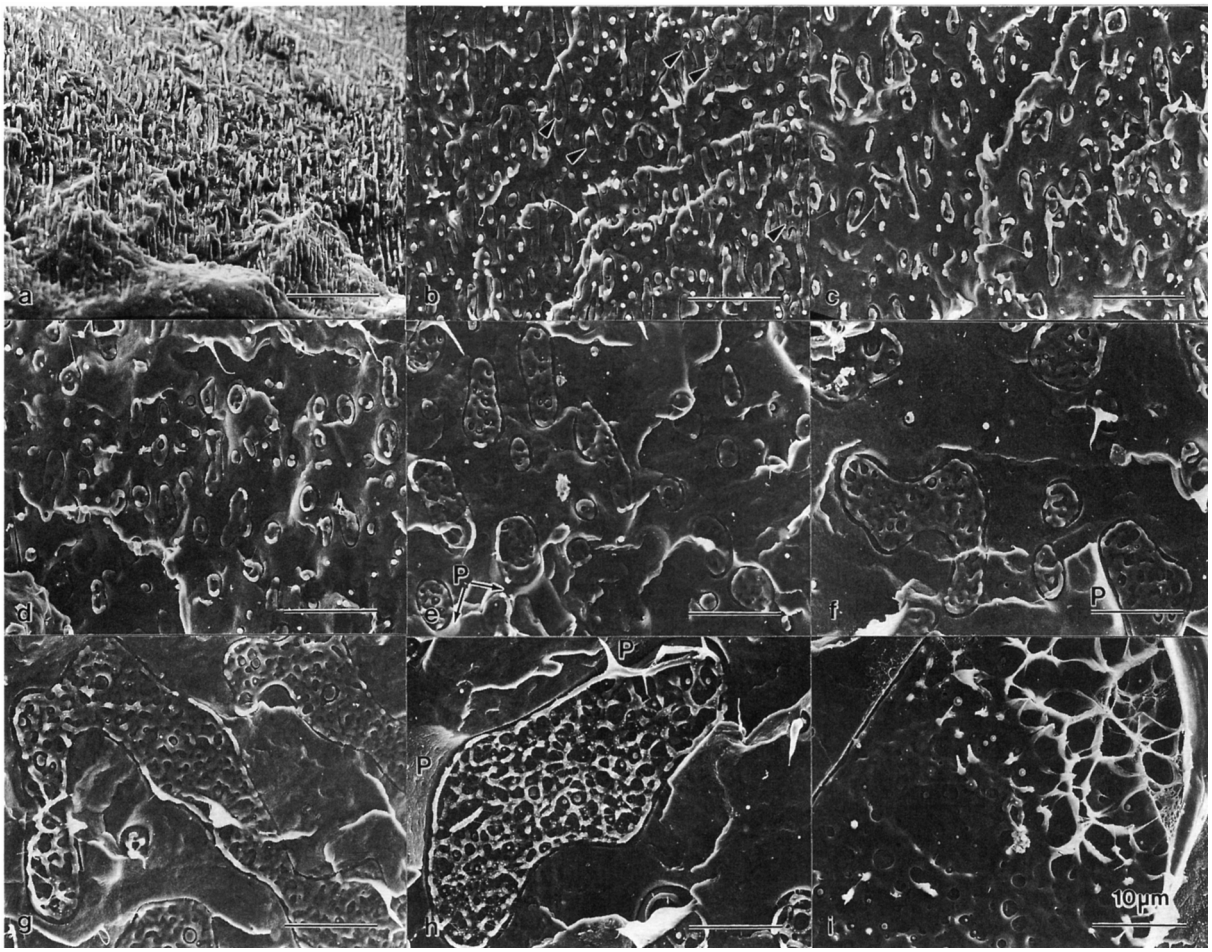

Figure 13 SEM images of the fractured surfaces of a 50PP/50LLDPE blend showing the progress of coalescence in the blend during remelting: (a) as-blended, and after being remelted for (b) 1 min, (c) 2 min, (d) 3 min, (e) 5 min, (f) 8 min, (g) 12 min, (h) 20 min, and (i) 2 h.

It is possible that iPP was entrapped by two LLDPE particles or iPP/LLDPE complexes when they move towards each other during coalescence following a mechanism similar to that described by Everett.[19] However, because these iPP/LLDPE complexes were rarely seen in the blends containing LLDPE dispersions, this entrapment mechanism was, therefore, considered to be trivial for the complex formation. It appeared that because of the high weight fraction of LLDPE in this blend the rounded LLDPE particles tended to be in contact with each other, leading to further coalescence between the particles. Once two LLDPE particles were in contact forming a dumbbell shape, the concave portion of the interface at the neck of the dumbbell would be highly unstable due to interfacial tension that drives the dumbbell-shaped body to become spherical. This reshaping tendency would promote further particle–particle contacts and, thus, coalescence. Once a large number of dispersed particles are in contact, a complex network will form that interpenetrates with the matrix.

The formation of pores in this blend seems to be a result of the significant change in dispersion morphology. As shown earlier, these pores started to form in the first few minutes of remelting where the lamellalike morphology changed into a morphology in which rounded iPP/LLDPE complexes containing entrapped spherical iPP particles were embedded in the matrix of iPP. It is known that the surface tension of a liquid droplet exerts an addition pressure to the liquid and the pressure is proportional to α/R, where α is the surface tension and R the radius of the droplet. In the as-blended specimen,

the microconstituents would not have been compressed by the interfacial tension apart from the edge regions of the lamellae. During remelting, the blend would experience a significant change in internal pressure in a short time as the morphology of dispersion changed dramatically, with the spherical iPP/LLDPE complexes being compressed by the additional pressure from their interfaces. The change in internal pressure on the microconstituents would cause reduction in volume for the compressed elements and lead to the formation of shrinkage pores when the iPP liquid cannot flow into the incipient pores in time. These pores may nucleate to form larger pores during further remelting treatment.

CONCLUSIONS

In order to study the dispersion stability of iPP/LLDPE blends, the fracture morphology of as-blended and remelted iPP/LLDPE blends of five different component ratios (i.e., 90PP/10LLDPE, 75PP/25LLDPE, 50PP/50LLDPE, 25PP/75LLDPE, and 10PP/90LLDPE), prepared by twin-blade mixing, was investigated by SEM. It was found that the dispersion morphologies of the two blends of the lowest minor component (i.e., 90PP/10LLDPE and 10PP/90LLDPE) were relatively stable through the remelting treatment, while the blend of 50PP/50LLDPE was highly unstable.

In the as-blended status, the blend of 50PP/50LLDPE consisted of lamellae-like iPP and LLDPE, whereas the other blends contained spherical particles of their minor components. During remelting, the lamellae dispersion morphology of the 50PP/50LLDPE blend changed dramatically into a morphology containing iPP/LLDPE complexes (i.e., domains of LLDPE with embedded spherical iPP particles), pores, and iPP matrix. This morphology formed in the first few minutes of remelting and evolved in further remelting where it formed an interpenetrating network between iPP/LLDPE complexes and iPP matrix with pores formed at the interfaces between the two components.

Coalescence of the spherical particles of the minor components for the rest of the blends was evident. The coalescence was nearly finished after the first 20 min of remelting. The results of an analysis of the coalescence process occurring in these blends appeared to support a theoretical prediction made by Fortelny and Kovar.

We would like to think Dr. Michael Mackay and Mr. Grant Hay of the Department of Chemical Engineering, the University of Queensland, for conducting the viscosity measurement of pure iPP and LLDPE for this work.

REFERENCES

1. F. P. La Mantia, Ed., *Recycling of Plastic Materials,* ChemTec Publishing, Canada, 1993.
2. Y. Liu and R. W. Truss, *J. Polym. Sci., Polym. Phys. Ed.,* to appear.
3. A. P. Plochocki, in *Polymer Blends,* D. R. Paul and S. Newman Eds., Vols. I and II, Academic, New York, 1978.
4. J. W. Barlow, and D. R. Paul, *Polym. Eng. Sci.,* **21,** 985 (1981).
5. Ph. Teyssié, R. Fayt, and R. Jérôme, *Makromol. Chem., Macromol. Symp.,* **16,** 41 (1988).
6. S. Wu, *Polymer,* **26,** 1855 (1985).
7. G. N. Avgeropoulos, F. C. Weissert, P. H. Biddison, and G. C. A. Böhm, *Rubber Chem. Technol.,* **49,** 93 (1976).
8. L. D'Orazio, R. Greco, C. Mancarella, E. Martuscelli, G. Ragosta, and C. Silvestre, *Polym. Eng. Sci.,* **22,** 536 (1982).
9. E. N. Kresge, D. J. Lohse, and S. Datta, *Makromol. Chem., Macromol. Symp.,* **53,** 137 (1992).
10. R. Holsti-Miettinen, J. Seppälä, and O. T. Ikkala, *Polym. Eng. Sci.,* **32,** 868 (1992).
11. L. A. Utracki and B. D. Favis, in *Handbook of Polymer Science and Technology, Vol. 4, Composites and Specialty Applications,* N. P. Cheremisinoff, Ed., Marcel Dekker, Inc., New York, 1989, p. 173.
12. R. S. Schotland, *Polym. Eng. Sci.,* **6,** 244 (1966).
13. W. Wenig, *Angew. Makromol. Chem.,* **74,** 147 (1978).
14. E. S. Sherman, *J. Mater. Sci.,* **19,** 4014 (1984).
15. R. A. Varin and D. Djokovic, *Polym. Eng. Sci.,* **28,** 1477 (1986).
16. X. Zhou and J. N. Hay, *Polymer,* **34,** 4710 (1993).
17. W. Chiang, W. Yang, and E. Pukánszky, *Polym. Eng. Sci.,* **32,** 641 (1992).
18. G. Serpe, J. Jarrin, and F. Dawans, *Polym. Eng. Sci.,* **30,** 553 (1990).
19. D. H. Everett, *Basic Principles of Colloid Science,* Chapt. 10, Royal Society of Chemistry, London, 1988, p. 146.
20. J. J. Elmendorp, Ph.D. Thesis, Delft Univ. Techn., The Netherlands, 1986.
21. I. Fortelny and J. Kovar, *Eur. Polym. J.,* **25,** 317 (1989).
22. M. von Smoluchowski, *Physik. Z.,* **17,** 557 (1916).
23. M. von Smoluchowski, *Physik. Z.,* **17,** 585 (1916).
24. M. von Smoluchowski, *Z. Physik. Chem.,* **92,** 129 (1917).

25. J. T. G. Overbeek, in *Kinetics of Flocculation, Colloid Science,* Vol. I, H. H. Kruyt, Ed., Elsevier, Amsterdam, 1952, p. 278.
26. J. Kovar, J. Velek, I. Fortelny, and P. Cefelin, *30th IUPAC International Symposium on Macromolecules,* Haag, 1985, p. 378.
27. I. Fortelny and J. Kovar, *Polym. Compos.,* **9,** 119 (1982).
28. T. Malavasic and V. Musil, *J. Therm. Anal.,* **34,** 503 (1988).
29. F. Rybnikar, *J. Macromol. Sci.-Phys.,* **B27,** 125 (1988).
30. L. A. Utracki, D. J. Walsh, and R. A. Weiss, in *Multiphase Polymers: Blends and Ionomers,* L. A. Utracki and R. A. Weiss, Eds., ACS Symposium Series 395, American Chemical Society, Washinton, DC, 1989, p. 1.
31. H. Frensch, P. Harnischfeger, and B.-J. Jungnickel, *ibid,* 1989, p. 101.
32. R. Greco, G. Mucciariello, G. Ragosta, and E. Martuscelli, *J. Mater. Sci.,* **15,** 845 (1980).
33. D. A. Blackadder, M. J. Richardson, and N. G. Savill, *Makromal. Chem.,* **182,** 1271 (1981).
34. G. Spadaro and G. Rizzo, *Eur. Polym. J.,* **25,** 1189 (1989).
35. B. Gross and J. Peterman, *J. Mater. Sci.,* **19,** 105 (1984).
36. J. Martinez–Salazar, J. M. Garcia Tijero, and F. J. Balta Calleja, *J. Mater. Sci.,* **23,** 862 (1988).
37. P. J. Carreau, *Trans. Soc. Rheol.,* **16,** 99 (1972).

Received April 27, 1995
Accepted November 7, 1995